Influence of fine-scale heterogeneity patterns on the large-scale behaviour of miscible transport in porous media

A. M. M. Elfeki[1], F. M. Dekking[2], J. Bruining[3] and C. Kraaikamp[2]

[1]*Department of Irrigation and Hydraulics, Faculty of Engineering, Mansoura University, Mansoura, Egypt (Current address: Hydrology and Ecology Section, Delft University of Technology, PO Box 5048, 2600 GA Delft, Delft, The Netherlands)*

[2]*Department of Applied Probability, Faculty of Information Technology and Systems, Delft University of Technology, PO Box 5031, 2600 GA Delft, Delft, The Netherlands*

[3]*Department of Applied Earth Sciences, Faculty of Civil Engineering and Geosciences, Delft University of Technology, PO Box 5028, 2600 GA Delft, Delft, The Netherlands*

ABSTRACT: An extensive series of numerical simulations on two-dimensional flow and miscible transport are carried out. The purpose of performing these simulations is to study the influence of fine-scale heterogeneity patterns (i.e. horizontal laminations, cross-bedding at 45° and 135°) with short range and long range correlation structure on large-scale behaviour of miscible transport in porous media. Synthetic heterogeneous structures have been generated using newly developed stochastic techniques (e.g. the coupled Markov chain method) to model the subsurface formations in various configurations, using realistic characteristics, and the tree-indexed Markov chain method to merge these heterogeneities at various scales. The results of the simulation are compared with simulations on a reference model of heterogeneity where there is no fine-scale heterogeneity. The simulations show that the variation in the fine-scale heterogeneity inside the large-scale lithological units has considerable impact on concentration distribution and the spreading of miscible plumes. The combination of the two stochastic techniques (the coupled Markov chain model and the tree-indexed Markov chain) is a useful tool to study multi-scale transport behaviour in heterogeneous media. The fine-scale heterogeneity enhances the mixing process, but the definition of an asymptotic giga-scopic dispersion at field scale is still questionable.

KEYWORDS: *heterogeneity, stochastic process, fluid flow, scale-up, dispersion (flow)*

INTRODUCTION

Subsurface formations are highly heterogeneous and their heterogeneity manifests itself at a multitude of scales. The simulation of fluid flow in two- and three-dimensional models of specific heterogeneity patterns has become an important tool in both the field of petroleum engineering for prediction of recovery efficiency (Haldorsen & Damsleth 1990) and the field of hydrogeology for the prediction of contaminant fate. Elfeki *et al.* (1996) have performed numerical experiments on single- and multiple-scale heterogeneous formations. In their experiments, they dealt with two scales of variability, the so-called macro- and mega-scales. The macro-scale variability addressed in their paper corresponds to the fine-scale heterogeneity presented here in this paper. The fine-scale heterogeneity they considered is a continuous stationary correlated Gaussian random field, with exponential auto-correlation function and normal probability density function of the logarithm of the hydraulic conductivity. However, the present paper focuses more on fine-scale heterogeneity patterns that are discrete in nature and have different bedding inclinations and where the hydraulic conductivity distribution is bimodal. This type of heterogeneity has been observed in field outcrops (e.g. Oude Maas deposit, The Netherlands: Van Beek & Koster 1972). Figure 1 shows this type of large-scale stratification in the Huesca outcrop, Spain.

The current work deviates from the classical approach of handling variability of hydraulic conductivity as a stationary random function (e.g. Dagan 1986). Instead, a new technique is used, the tree-indexed Markov chain, to characterize heterogeneity patterns at various scales. The tree-indexed Markov chain has been developed by Dekking *et al.* (1999*a*) for general purpose image analysis. It has been adapted for subsurface characterization. This new technique is investigated as a tool to merge information from various scales to study the behaviour of fine-scale heterogeneity patterns on large-scale prediction of miscible transport in porous media.

GENERATION OF LARGE-SCALE AND FINE-SCALE HETEROGENEOUS STRUCTURES

The coupled Markov chain model, developed by Elfeki (1996) and extended by Elfeki & Dekking (2001) to conditioning on multiple wells, is used to generate synthetic data which mimic,

Presented at the 7th European Conference on the Mathematics of Oil Recovery, Italy, September 2000.

1354-0793/02/$15.00

Fig. 1. Huesca outcrop, Spain, showing the large-scale stratification (courtesy of Cees Geel).

in some sense, the heterogeneity pattern of the Oude Maas deposit (Van Beek & Koster 1972) for flow and transport experiments. A brief description of the coupled Markov chain model is given below. The model is a stochastic technique that couples two chains. The first one is used to describe the sequence in lithology in the vertical direction, and the second chain describes the sequence of variation in the lithological structure in the horizontal direction. The two chains are coupled in the sense that a state of a cell in the domain is dependent on the state of two cells, the one on top and the other on the left of the current cell. This dependence is described in terms of transition probabilities from the two chains. The coupled Markov chain technique is efficient in terms of computer time and storage in comparison with other techniques available in the literature (see Elfeki *et al.* (1995) for details).

Figures 2 and 3 (left and middle columns) show images generated by the coupled Markov chain model. For simplicity one pixel is equated with one metre square, which is not necessarily realistic from the geological point of view. However, the method easily adapts to any scale. Sample input parameters (transition probabilities) for generating the large-scale structure (left top corner image in Figure 2) are presented in Table 1. This large-scale structure is considered as a reference model for the subsurface formation in the study. The large-scale heterogeneity pattern is a layered reservoir with slight inclination. This shape is frequently encountered in field observations. The geological system is assumed to consist of two different lithologies that appear in black and white. The elements of the transition probability matrix for the horizontal direction, p^{H}_{ij} (which means the probability of a given lithology, *i,* is following

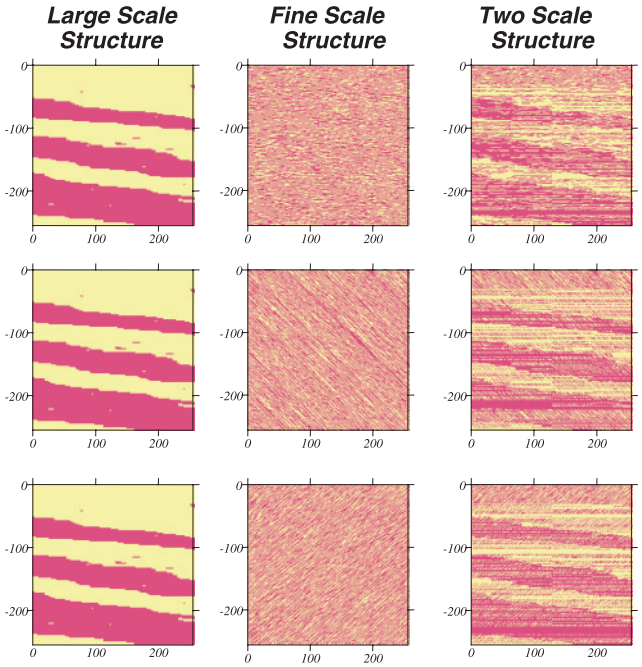

Fig. 2. Merging large-scale structure (left column) with fine-scale structure with short-range correlation (middle column) to simulate two-scale structure (right column). Image resolution is 256 × 256. The dimensions are in metres.

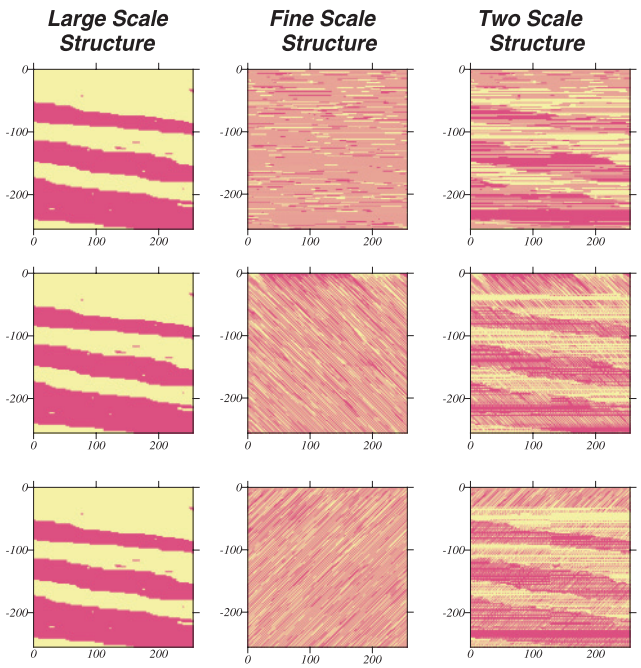

Fig. 3. Merging large-scale structure (left column) with fine-scale structure with short-range correlation (middle column) to simulate two-scale structure (right column). Image resolution is 256 × 256. The dimensions are in metres.

Table 1. *Input parameters to generate the large-scale structure in Figures 2 and 3 (left column)*

Horizontal transition probability matrix			Vertical transition probability matrix		
State	*B*	*W*	State	*B*	*W*
B	0.98	0.02	*B*	0.80	0.20
W	0.02	0.98	*W*	0.20	0.80

another lithology, *j*), are given in Table 1 (e.g. $p^{H}_{BB} = 0.98$ and $p^{H}_{BW} = 0.02$ and so on). A similar transition probability matrix is used in the vertical direction with p^{V}_{ij} (e.g. in Table 1 $p^{V}_{BB} = 0.80$ and $p^{V}_{BW} = 0.20$ and so on).

The method can model any fine-scale structure within the large structure (Dekking *et al.* 2001). Here, we confine ourselves to a single fine structure in the large-scale structure. The fine-scale heterogeneity patterns considered in the simulation are:

1. fine-scale horizontal lamination with short range (Fig. 2 top row, middle image) and long range (Fig. 3 top row, middle image) correlation in the horizontal direction;
2. inclined bedding at 45° with short range (Fig. 2 middle row, middle image) and long range (Fig. 3 middle row, middle image) correlation in the bedding direction;
3. inclined bedding at 135° with short range (Fig. 2 bottom row, middle image) and long range (Fig. 3 bottom row, middle image) correlation in the bedding direction.

Variogram analysis of fine-scale patterns shows that the correlation lengths in the case of the short-range correlation structure are 3.4 m and 0.71 m in the direction of the bedding and perpendicular to it, respectively. In the case of the long-range correlation structure the correlation length in the bedding direction does not exist (the variogram is not bounded) and the correlation length is about 0.71 m perpendicular to the bedding.

MERGING LARGE-SCALE AND FINE-SCALE HETEROGENEITIES

A tree-indexed Markov chain developed by Dekking *et al.* (1999*a*) is used to merge fine-scale heterogeneity with large-scale heterogeneity. This methodology was originally developed for general-purpose image analysis (see Dekking *et al.* 1999*b*), and adapted for characterization of subsurface heterogeneity by Dekking *et al.* (2001). The methodology is based on a coarse- to fine-scale representation of the heterogeneous structures indexed by nodes on lattices that are summarized on trees. Different depths in the tree correspond to different spatial scales in representing the heterogeneous structures. On these trees a Markov chain is used to describe scale-to-scale transitions and to account for the uncertainty in the stochastically generated images. This is discussed in more detail below.

A two-dimensional image can be represented by K scales (levels). At a particular level, L_M, such that $0 \leq M \leq K$, the corresponding number of nodes (pixels) at this scale is $2^M \times 2^M$. There is a factor 4 between the number of grid cells at each scale and the previous coarser one. This yields the quad tree structure over all scales of an image. The procedure is simply based on the successive subdivision of an image into four equal-sized quadrants. The simplest case is that of binary images, which contain only black and white colours. If a binary image contains both blacks and whites, it is declared grey (a new colour), and divided into four sub-quadrants, and so on, until quadrants are obtained that consist entirely of blacks or entirely of whites. Figure 4 shows a resolution of an image by this procedure (for details see Samet (1990)).

Images can be randomized by randomizing the process of replacing quadrants by sub-quadrants: if a quadrant is grey the four sub-quadrants obtain their colours randomly according to a distribution that depends on the level, on the position of the quadrant and on the colours of the neighbours of the quadrant. One can consider these distributions as the transition probabilities of an inhomogeneous Markov chain on the quad tree. In applications, one estimates the transition probabilities from a set of images (see Dekking *et al.* 1999*a* for details).

It has been shown by Dekking *et al.* (2001) that quad trees are not suited for geological applications because of vertical discontinuities. This phenomenon is practically avoided by the use of dyadic trees. In the dyadic tree, there is a factor of 2 between any scale and the previous coarser one. In this representation any node in the tree has two descendent nodes at the next finer scale and one parent node at the preceding coarser scale. The tree is used to perform separately scaling in the vertical direction (V-scaling) and to perform scaling in the horizontal direction (H-scaling). First, the image is decomposed into its corresponding scales in the vertical direction by a dyadic tree with K_V levels until the pixel level in the vertical direction is reached (we call this the pixel line). Second, the features that do not appear in the vertical direction will appear when the scaling in the horizontal direction is performed. The strips that appear in a grey colour are scaled horizontally in K_H steps in the horizontal direction until the pixel level is reached.

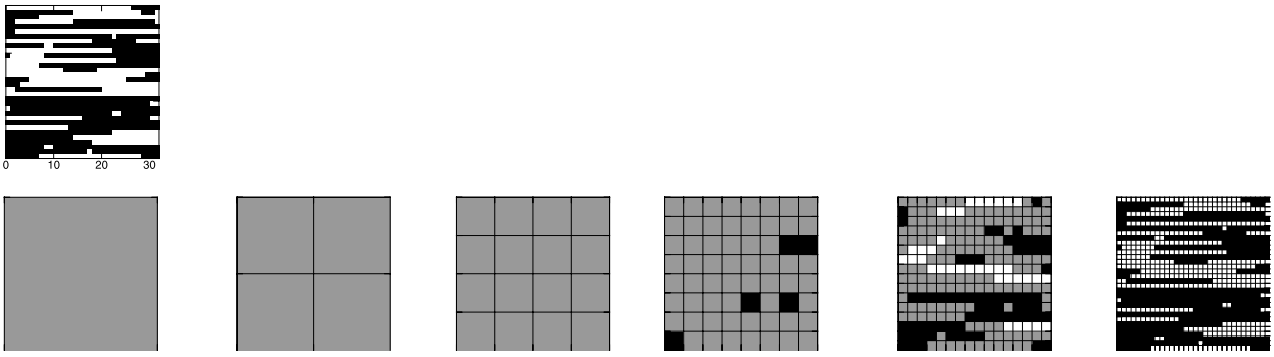

Fig. 4. Scale resolution of an image with 32 by 32 pixels ($K = 5, N = 32$, left top of the figure is the image, bottom row is scales $M = 0,1,2,3,4$and5 respectively from left to right).

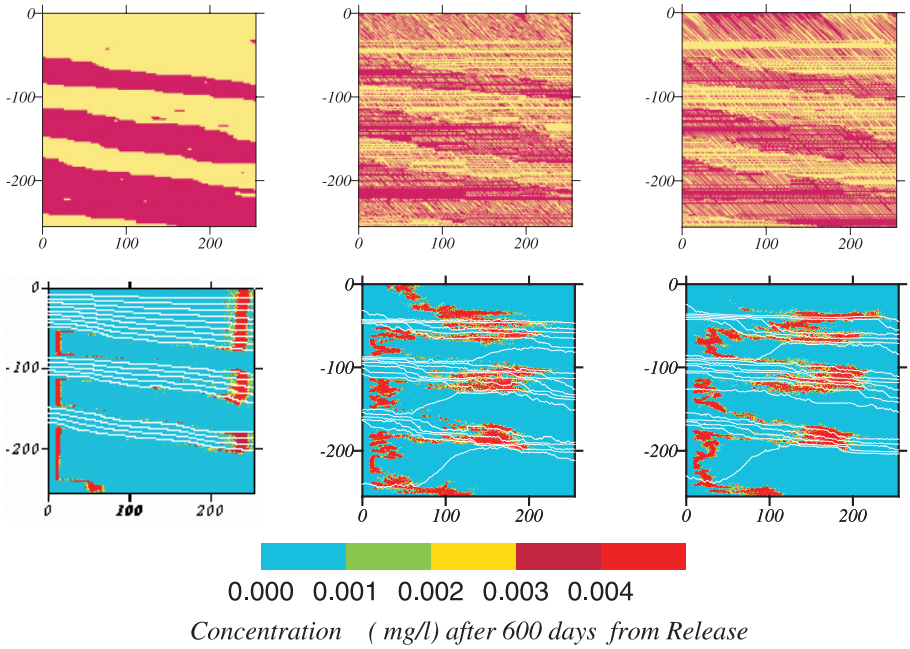

Fig. 5. Flow and transport simulations in three types of heterogeneity: left column, homogeneous layers (reference model: large-scale structure); middle column (two-scale model: fine-scale structure with inclined bedding at 45° with short range correlation imbedded in the large-scale structure); right column (two-scale model: fine-scale structure with inclined bedding at 45° with long range correlation embedded in the large-scale structure).

SINGLE PHASE FLOW AND MISCIBLE TRANSPORT EXPERIMENTS

The procedure to simulate single phase flow and miscible transport experiments involves a number of steps.

1. The large-scale and fine-scale heterogeneities are generated using the coupled Markov chain technique.
2. The tree-indexed Markov chain is used to merge the two different types of heterogeneity and produce a two-scale structure (Fig. 5).
3. Hydraulic conductivity values are assigned to each geological material. In the present study, values of 100 m day^{-1} and 1 m day^{-1} are used for high and low conductivity zones respectively.
4. The single-phase flow equation is solved numerically by the finite difference scheme with constant hydraulic head at the left and right boundaries (left $H_l = 1$ m and right $H_r = 0$ m), while the top and bottom boundaries are considered as no flow boundaries.
5. The specific discharge and the real water velocity are related to the effective porosity. We put the porosity n equal to 1 because the porosity only serves as a rescaling for time.
6. The miscible transport equation is solved numerically using the random walk technique (Uffink 1990). A set of particles is released from a strip source in the upstream part of the domain. Initially no solutes are present. 100 g solutes are injected in a strip with dimensions 1 m in the flow direction and 250 m perpendicular to it. The centre of the source is located at (10 m, −128 m) from the top left corner of the flow domain. Each particle moves with an advective component along the streamline and a dispersive component according to the pore-scale dispersion process with longitudinal dispersivity of 0.1 m in the flow direction and a lateral dispersivity of 0.01 m perpendicular to the flow direction.
7. The plume statistics such as the centroid of the particle cloud, spreading of the plume around its centroid, macrodispersion coefficient, plume angle of rotation and breakthrough curve at 190 m from the solute source are calculated each time step.

DISCUSSION OF RESULTS

The plume statistics are presented in Figures 6–8. Figure 6 (top) shows the centroid displacement (first-order moment of the particle cloud) in time. From the x-component, one would recognize that the plume moves at a slower rate in the case of two-scale heterogeneity in comparison with the reference model (large-scale structure without fine-scale heterogeneous structure). This is because of the tortuous paths generated by the fine-scale heterogeneity. The degree of slowness increases in the following order: long horizontal lamination, short horizontal lamination, bedding at 45° with long correlation and with short correlation and bedding at 135° with short and long correlations respectively. The y-component of the centroid moves the most to the bottom in the case of bedding at 45° with long correlation.

Plume spreading (second-order moment of the particle cloud) is displayed in Figure 6 (bottom). The longitudinal second moment grows faster than it does linearly in time showing super-diffusive regime in the reference model. Including fine-scale heterogeneity resulted in less super-diffusivity. The degree of super-diffusivity decreases in the following order: long horizontal laminations, bedding at 45° with long correlation, bedding at 135° with long correlation, short horizontal laminations, bedding at 45° with short correlation and bedding at 135° with short correlation, respectively. This can be explained by the fact that the more a structure deviates from a homogeneous layered structure the less super-diffusivity will occur. The lateral second moment of the plume decreases the most in the case of bedding at 45° with long correlation. The bedding direction in the top layer is contributing in squeezing the plume laterally.

The angle of rotation of the plume is displayed in Figure 7 (top). The angle of rotation is calculated by $\theta = 2 \tan^{-1}\{2\sigma^2_{xy}/(\sigma^2_{xx} - \sigma^2_{yy})\}$, where, σ^2_{xx} is the longitudinal variance of the particle displacements around their centroid, σ^2_{yy} is the transverse variance of the particle displacements around their centroid, and σ^2_{xy} is the cross-covariance of the particle displacements (Tompson & Gelhar 1990). The

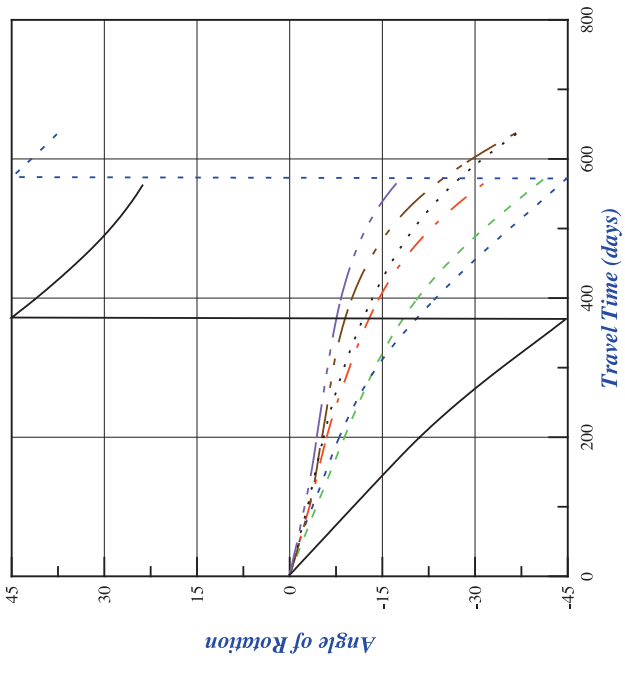

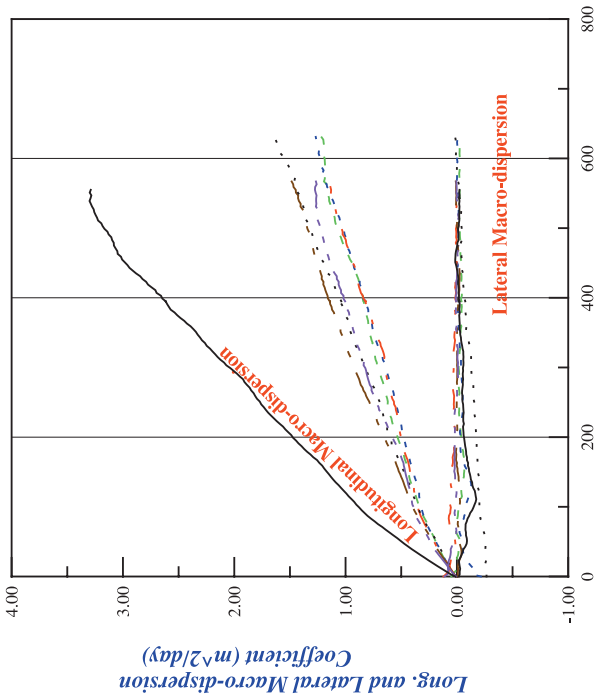

Fig. 7. Plume statistics (2): top graph is evolution of angle of rotation of the plume with respect to the x-direction versus time; bottom graph is evolution of macro-dispersion coefficient versus time.

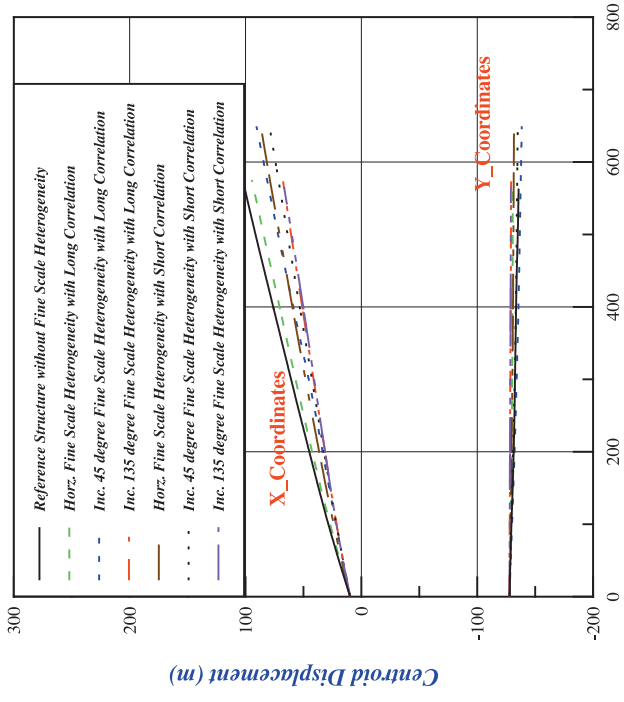

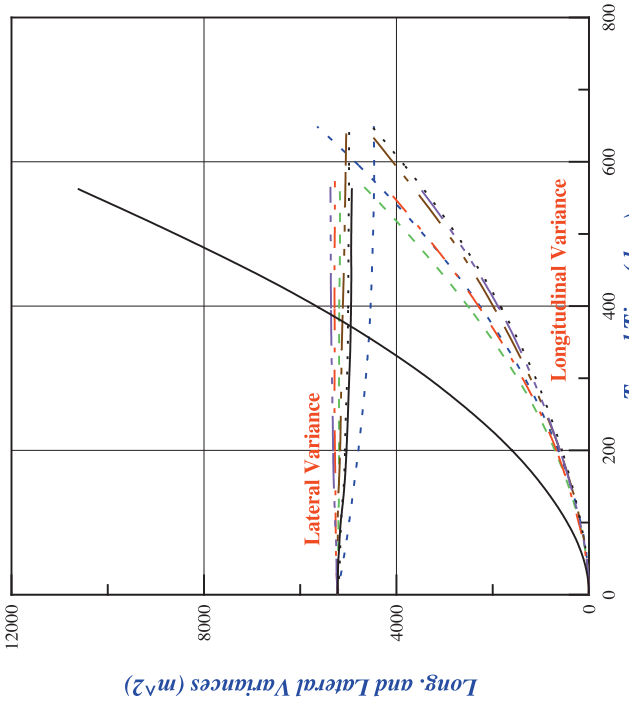

Fig. 6. Plume statistics (1): top graph is the plume centroid displacement versus time; bottom graph is plume second spatial moments versus time.

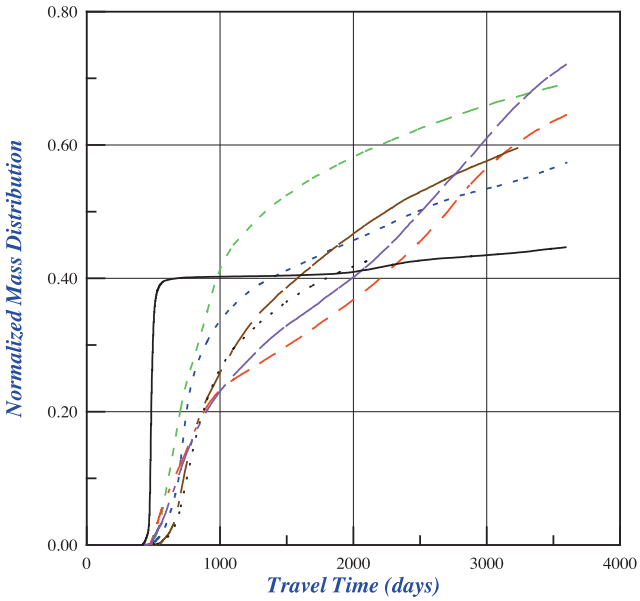

Fig. 8. Breakthrough curves at $x = 200$ m from the origin.

plume angle of rotation shows the change of orientation of plume in time with respect to the x-axis. In the reference model the plume angle of rotation decreases. After about 380 days the longitudinal spreading reaches the lateral spreading (i.e. $\sigma^2_{xx} = \sigma^2_{yy}$). In the case of the fine-scale structure at 45° with long range correlation this occurs after about 580 days, a delay of about 200 days. This delay is, of course, due to the fine-scale heterogeneity. The same behaviour at different delay times for the different heterogeneous patterns is expected to occur.

Figure 7 (bottom) displays the growth of the macro-dispersion coefficient in time. The macro-dispersion coefficient is defined as half the derivative of the variance of the particle cloud. Moment calculations can only be performed until the first particle leaves the domain of interest. In our calculations this takes place after about 600 days. For the computation of the breakthrough curve times after 600 days are still relevant. An asymptotic giga-dispersion coefficient does not exist. Fine-scale heterogeneity leads to a smaller longitudinal macro-dispersion coefficient in comparison with the reference model. At a time of 600 days a longitudinal macro-dispersion of 3.5 $m^2\,day^{-1}$ is reached at the reference model. However, in the two-scale models an average value of 1.5 $m^2\,day^{-1}$ is obtained. This means that the fine-scale heterogeneity leads to a reduction of the dispersion coefficient to about a half within the time limit of the particle cloud that stays within the flow domain. The discrepancies of the longitudinal dispersion coefficient for the different patterns are within a range of 1.5 $m^2\,day^{-1}$ to 1.2 $m^2\,day^{-1}$ at 600 days. The lateral macro-dispersion coefficient is practically zero which has been confirmed by earlier Monte-Carlo analysis performed by Elfeki (1996).

Breakthrough curves, at 200 m from the left side of the domain, are plotted in Figure 8. After 2000 days since release, about 40% of the injected mass is recovered in the reference model. In the case of the fine-scale structure at 135° degrees with both long and short-range correlations the percentage recovered is slightly less than 40%. This is due to the bedding angle that is against the global flow direction. However more than 40% is recovered in case of horizontal laminations and bedding at 45°. The long-range horizontal lamination displays the maximum percentage recovered, that is, about 60% after 2000 days. This results from the preferential connected paths of the long-range horizontal laminated bedding. One should also notice that the curves in Figure 8 display different shapes for each type of fine-scale heterogeneity, however, these shapes show the same behaviour for the same type of heterogeneity with different correlation.

CONCLUSIONS

1. The first goal of this work was to investigate the usefulness of using a new technique that is called 'tree-indexed Markov chains' to address fine and large scales of information. It has been shown that the method is capable, in a systematic way, of incorporating various fine-scale patterns in large-scale structures. Further work is needed to handle more than two scales and more than two geological materials. Extension to 3D structures is not hard, except when conditioning to multiple well data is required.
2. The second goal was to understand the influence of fine-scale heterogeneity patterns on the large-scale mixing of pollutants in porous formations. The present 2D simulation study has shown that the variation in fine-scale heterogeneity pattern has impacts on large-scale transport behaviour. Relative to the reference model (large-scale structure without fine-scale heterogeneity), it has been shown that fine-scale heterogeneity causes slower and more dispersive plumes (reduction of the super-diffusivity in the tilted layered system considered here as a reference model, however, an asymptotic giga-dispersion does not exist) and a reduction of the longitudinal macro-dispersion coefficient to about a half within the time limit of the experiments (600 days). However, there is no significant impact on the statistics of the plume as far as various patterns of fine-scale heterogeneity are concerned. With respect to recovery, fine-scale heterogeneity enhances recovery compared to the reference model.
3. Similar studies on the effect of other types of internal fine-scale structures with different degrees of contrasts are recommended to give information on a broad range of various heterogeneous patterns that exist in nature.

This study was financially supported by the DIOC project 'Shallow Subsurface' of Delft University of Technology, Delft, The Netherlands.

REFERENCES

Dagan, G. 1986. Statistical theory of Groundwater Flow and Transport: Pore to Laboratory. Laboratory to Formation and Formation to Regional Scale. *Water Resources Research*, **22**, 9, 120S–134S.

Dekking, F.M., Kraaikamp, C. & Schouten, J.G. 1999a. Binary images and inhomogeneous tree-indexed Markov chains. *Revue Roumaine Math. Pures Appl.*, **44**, 181–188.

Dekking, F.M., Kraaikamp, C., Elfeki, A.M. & Bruining, J. 1999b. Synthesis and simulations of digital images by tree-indexed Markov chains. *Proceedings of SPIE International Society for Optical Engineering*, **3815**, SPIE, Denver, Colorado, 227–238.

Dekking, F.M., Elfeki, A.M.M., Kraaikamp, C. & Bruining, J. 2001. Multi-Scale and Multi-Resolution Stochastic Modelling of Subsurface Heterogeneity by Tree-indexed Markov chains. *Computational Geosciences*, **5**, 47–60.

Elfeki, A.M. & Dekking, F.M. 2001. A Markov Chain Model for Subsurface Characterization: Theory and Applications. *Mathematical Geology*, **33**, 5, 569–589.

Elfeki, A.M.M., Uffink, G.J.M. & Barends, F.B.J. 1996. Solute Transport in Single and Multiple Scale Heterogeneous Formations: Numerical Experiments. *In:* Soares, A., Hernandez, J. & Froidevaux, R. (eds) *geoENV 96, First European Conference on Geostatistics for Environmental Applications, Lisbon, Portugal.* Kluwer Academic Pub., 51–63.

Elfeki, A.M.M. 1996. *Stochastic characterization of geological heterogeneity and its impact on groundwater contaminant transport*. Ph.D. Thesis, Delft University of Technology, Delft, The Netherlands.

Elfeki, A.M.M., Uffink, G.J.M. & Barends, F.B.J. 1995. Stochastic simulation of heterogeneous geological formations using soft information, with an application to groundwater. *In:* Kovar, K. & Krasny, J. (eds) *Groundwater Quality: Remediation and Protection, GQ'95*. IAHS Publication No. **225**.

Haldorsen, H. & Damsleth, E. 1990. Stochastic Modelling. *Journal of Petroleum Technology*, **42** (4) 127–139.

Samet, H. 1990. *Applications of Spatial Data Structures*. Addison-Wesely Publishing Company. Inc, Reading.

Tompson, A.F.B. & Gelhar, L.W. 1990. Numerical Simulation of Solute Transport in Three-dimensional, Randomly Heterogeneous Porous Media. *Water Resources Research*, **26** (10), 2541–2562.

Uffink, G.J.M. 1990. *Analysis of Dispersion by The Random Walk Method*. Ph.D. Thesis, Delft University of Technology, Delft, The Netherlands.

Van Beek, J.L. & Koster, E.A. 1972. Fluvial and Esturarine Sediments Exposed Along The Oude Maas (The Netherlands). *Sedimentology*, **19**, 237–256.

Received 2 January 2001; revised typescript accepted 11 January 2002